Conformation of some amylose triesters: The influence of side groups*

P. Zugenmaier† and H. Steinmeier
Institut für Physikalische Chemie der TU Clausthal, Adolf-Römer-Strasse 2A, D-3392 Clausthal-Zellerfeld, FRG
(Received 4 November 1985; revised 13 January 1986)

The conformation of five amylose triesters, namely amylose triacetate II (ATAII), tripropionate (ATP), tributyrate (ATB), triisobutyrate (ATisoB) and trivalerate (ATV), have been determined by an X-ray study combined with a conformational analysis. The conformation of the homologous series from ATP, ATB to ATV with prolongation of the ester group by a methylene unit exhibits left-handed 5-fold helices. However, the change of the side group to a bulkier shape from ATB to ATisoB forces the main chain conformation from a 5/4 to a left-handed 4-fold (4/3) helix. The conformation of ATAII is close to a 9/7 helix.

(Keywords: amylose triesters; preparation; X-ray diffraction; conformation of single chains; side-group effect)

INTRODUCTION

The first detailed structural analysis of a polysaccharide derivative was successfully performed by Sarko and Marchessault[1] on amylose triacetate (ATAI) in 1966. Since then, the structure of different amylose modifications, of amylose ethers and of solvent complexes have been extensively investigated by improved techniques and the results summarized in a review[2]. However, the structure of the high-temperature modification of amylose triacetate (ATAII) has remained unsolved, although good fibre X-ray patterns were obtained by Sarko[3]. He proposed a 7-fold helix but no further conformational studies were performed. This helix has a fibre repeat of ~17 Å with a rise per residue of 2.4 Å, which is far below the values of 3.6 to 4.1 Å later found for other amylose derivatives. The conformation of further amylose esters, which might also give some hints on the conformation of ATAII, has not yet been solved.

An attempt has been undertaken to synthesize the homologous esters amylose tripropionate (ATP), amylose tributyrate (ATB), amylose triisobutyrate (ATisoB) and amylose trivalerate (ATV) and to solve the conformation of a single chain by X-ray and conformational analysis. Such a homologous series can also be used to study the influence of the length and shape of the side chain on the helix backbone, which has so far been considered negligible for most polymers.

EXPERIMENTAL

The amylose esters investigated in this study were produced by homogeneous esterification with the corresponding acid anhydride. The general method of derivatization is the same for all amylose triesters[11]. Commerically available Avebe amylose that was precipitated in butanol was used in this study. Potato and corn amylose from various commercial sources without any further purification led to the same results for amylose tripropionate.

Amylose (2 g) was suspended in formamide (40 ml) at 80°C. Pyridine (40 ml) was added at 40°C after the amylose had been completely dissolved. Acid anhydride (0.5 mol) was added dropwise under stirring. The reaction medium was further stirred for 12 h at 60°C and the reaction product then precipitated by pouring the mixture into ice–water. The partially esterified product was obtained through filtration.

The triester was produced in a second step. The partially substituted compound was redissolved in a solution of pyridine (20 ml) and acid anhydride (20 ml). The reaction mixture was stirred for 24 h at 60°C and the product isolated as described above. It was then washed free of acid and pyridine with water, dissolved in chloroform, reprecipitated in ether and dried in vacuum. The final product was a fine white powder.

The degree of substitution (*DS*) was determined by infra-red analysis and was higher than 2.9 for all the esters synthesized.

The experimental densities measured by the flotation method, the calculated values with the unit cells determined by X-ray diffraction (see below) and the melting temperatures obtained by differential scanning calorimetric (d.s.c.) experiments are summarized in *Table 1*. The melting temperature decreases with increasing

Table 1 Experimental (ρ_{ex}) and calculated (ρ_{cal}) density and melting temperature (d.s.c.) T_m of different amylose triesters

	ρ_{ex} (g cm^{-3})	ρ_{cal} (g cm^{-3})	T_m (K)
ATAII	1.31	1.25	575
ATP	1.26	1.25	504
ATB	1.23	1.20	437
ATisoB	1.18	1.17	478
ATV	1.13	1.12	418

* Dedicated to Prof. Dr W. Ruland on the occasion of his 60th birthday.
† To whom correspondence should be addressed.

0032-3861/86/091601-08$03.00

length of the side chains, as expected. Oriented crystalline fibres of the amylose triesters for X-ray studies were produced by stretching films of the various compounds, which were cast from solutions in acetone, and drawn in a hot air stream to about four times the original length. These fibres showed good orientation and high crystallinity, which was further improved by annealing the fibres just below the melting temperature for about 10–20 min. The crystalline polymorph of amylose triacetate II (ATAII) was produced by annealing the normally obtained polymorph ATAI at 240°C in glycerol.

Table 2 Unit cell characteristics for different amylose triesters, amylose triacetate II (ATAII), tripropionate (ATP), tributyrate (ATB), trisiobutyrate (ATisoB) and trivalerate (ATV): unit cell parameters a, b and c ($\alpha=\beta=\gamma=90°$), unit cell volumes V and number of chains through unit cell N

	a (Å)	b (Å)	c (Å)	V (Å^3)	N
ATAII	29.04	29.97	34.00	20705	6
ATP	20.26	35.10	18.46	13127	6
ATB	22.04	38.18	18.45	15525	6
ATisoB	32.38	32.38	16.10	16880	8
ATV	23.44	27.85	18.80	12272	4

The X-ray investigations were carried out with Ni-filtered CuKα radiation using a flat film camera in a vacuum chamber.

CaF_2 powder served for calibration purposes and gave a Debye–Scherrer ring on the fibre pattern with a spacing of 3.155 Å. The unit cell parameters were determined by evaluating the fibre diagrams and refined by a least-squares method. *Table 2* shows the refined unit cell dimensions a, b and c with $\alpha=\beta=\gamma=90°$, the volume of unit cells and the number of chains running through each unit cell. The conformations were calculated and analysed with a computer program, which is described in detail in previous publications[4].

RESULTS AND DISCUSSION

The homologous series of amylose esters, amylose triacetate II (ATAII), tripropionate (ATP), tributyrate (ATB), triisobutyrate (ATisoB) and trivalerate (ATV), are easily available derivatives of amylose. Fibre X-ray diagrams were obtained for all the produced amylose esters and are shown in *Figure 1*. The unit cells determined by indexing the fibre X-ray patterns are

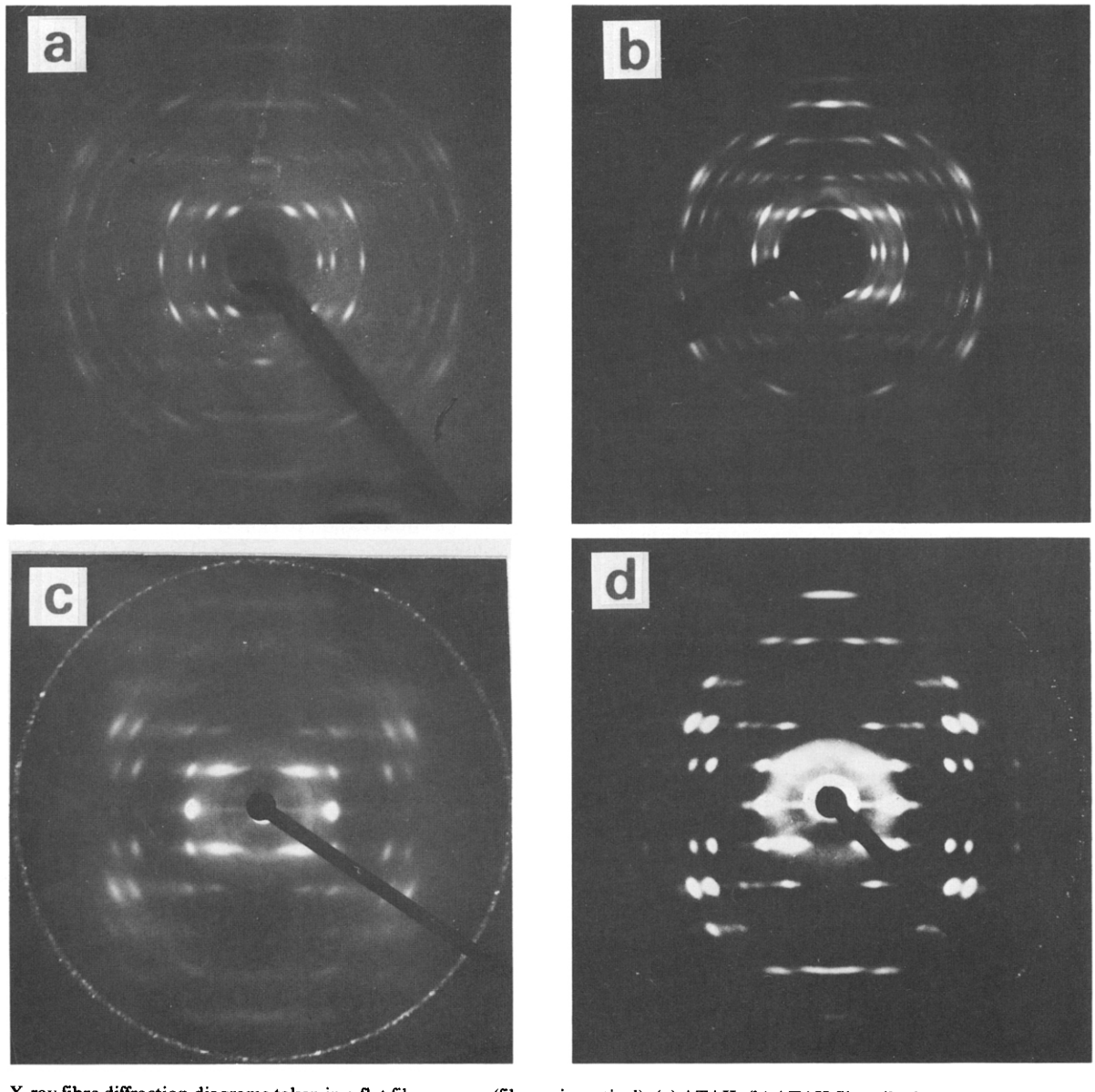

Figure 1 X-ray fibre diffraction diagrams taken in a flat film camera (fibre axis vertical): (a) ATAII, (b) ATAII fibre tilted 13°, (c) ATP, (d) ATP fibre tilted 12°

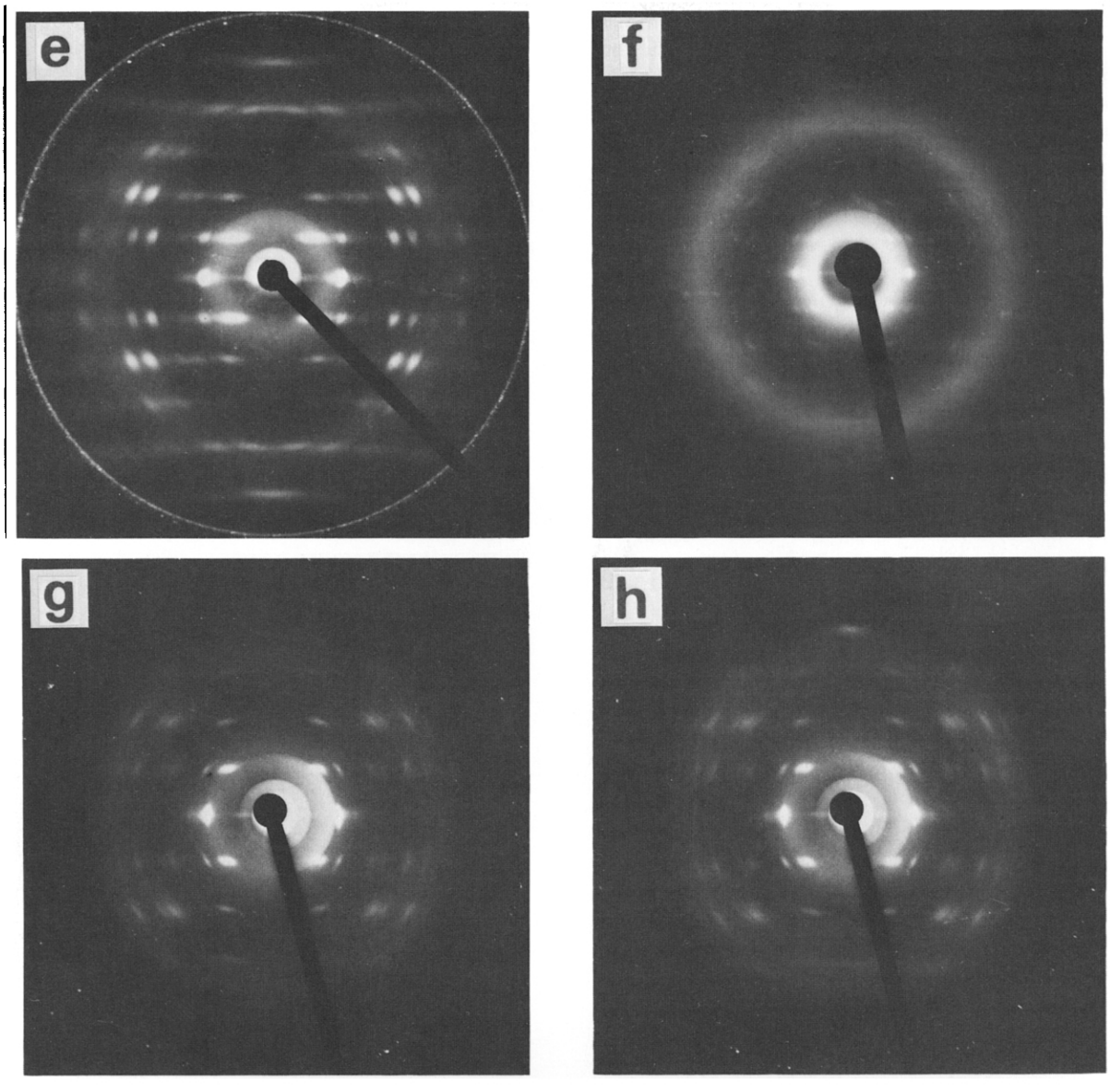

Figure 1 (continued) (e) ATB, (f) ATV, (g) ATisoB, (h) ATisoB fibre tilted 11°

summarized in *Table 2* with the unit cell volume and the number of chains passing through the unit cell. A first attempt to solve the structure of ATB failed in 1946[5]. Only the fibre repeat was determined as $c = 14.9$ Å, which is not comparable with the result in this study, $c = 18.45$ Å.

All amylose esters investigated form orthorhombic lattices with $a = b$ for ATisoB and $a \neq b$ for all the others. The ratio b:a for ATP and ATB suggests a quasi-hexagonal unit cell. A meridional reflection on the fifth layer line for ATP, which is clearly detected on an X-ray diagram from a tilted fibre, leads to the proposal of a 5-fold helix for the conformation of this polysaccharide derivative. This proposal is confirmed by density measurements of an ATP fibre (*Table 1*). The experimental density can be matched with the calculated one by assuming six chains consisting of 5-fold helices running through the unit cell. Fibres of ATB and ATV tilted to the fifth meridional reflection did not produce a clear meridional reflection. The conformations of the chains were also interpreted as 5-fold helices as for ATP because of the close resemblance in fibre repeat and agreement in calculated and measured density (*Table 1*).

The X-ray pattern of ATisoB shows a meridional reflection on the fourth layer line by adequate tilting of the fibre. A 4-fold helix is proposed and confirmed by density considerations. The fibre repeat distance as well as a quasi-tetragonal unit cell, frequently found in other amylose derivative[6] crystals, support a 4-fold helix.

The X-ray diagram of a 13° tilted fibre of ATAII (*Figure 1b*) reveals a ninth-order meridional reflection. The complete pattern can be indexed with an orthorhombic unit cell, $a = 28.04$ Å, $b = 20.97$ Å, c (fibre repeat) $= 34.0$ Å, in which the base plane (a,b) has the same size as the one proposed by Sarko[3] but the c dimension is now doubled. The conformation of the chain backbone can be approximated by a 9-fold helix and the experimentally determined density calculated. However, the existence of fourth- and eighth-order meridional reflection points to a deviation from an exact 9-fold helix. Every second layer line is extinguished in the X-ray diagram.

Models for the different conformations can be established through a conformational analysis[4] and the different helices verified. The main-chain conformation was calculated with a flexible ring while the side-group conformation was refined with variable torsion angles

only. Results were used from earlier conformation studies, where only left-handed 4-fold helices have been found. The present investigation leads to left-handed 5-fold (5/4) helices for ATP, ATB and ATV, to a left-handed 4-fold (4/3) helix for ATisoB and to a left-handed 9-fold (9/7) helix for ATAII. The atomic coordinates for a low-energy conformation of the three different kinds of helices are listed in *Tables 3–5*. The atomic coordinates for ATB and ATP can be approximated by shortening the conformation of ATV by a methyl or an ethyl group, respectively.

Projections of the chain molecules of all five esters onto two planes are depicted in *Figures 2–4* and represent the shape of the different conformations with various lengths of side groups. Characteristic values of the helices of amylose esters investigated in this study and, for comparison, similar helices for further derivatives are collected in *Table* 6. All chains of amylose derivatives in the crystalline state form left-handed between 4- and 5-fold helices. The type of helix can be correlated with the size of the fibre repeat. Left-handed 4/3 helices correspond to a fibre repeat c between 15.4 and 16.1 Å, 5/4 helices to a c of approximately 18.5 Å. The rise per residue of all

Table 3 Cartesian coordinates (in Å) of basic residue of ATV (5/4 helix)

	X	*Y*	*Z*
O4	0.000	−2.025	0.000
C1	−2.794	−1.493	3.025
C2	−2.186	−2.884	2.910
C3	−0.928	−2.885	2.065
C4	−1.229	−2.256	0.701
C5	−1.907	−0.898	0.869
C2A	−2.599	−4.678	4.405
C2'M	−2.230	−5.194	5.760
C2''M	−2.919	−6.550	5.999
C2'''M	−2.539	−7.081	7.393
C2''''M	−3.228	−8.438	7.631
C3'M	0.688	−6.152	2.525
C3''M	1.686	−6.678	3.573
C3'''M	1.995	−8.160	3.291
C3''''M	2.992	−8.686	4.339
C6'M	−4.929	−2.071	−2.528
C6''M	−6.133	−1.557	−3.339
C6'''M	−6.817	−2.740	−4.049
C6''''M	−8.021	−2.228	−4.860
O2	−1.999	−3.489	4.186
O3	−0.468	−4.241	1.885
O5	−3.066	−1.022	1.719
O6	−3.207	−1.360	−1.125
O2A	−3.320	−5.214	3.612
O3A	0.843	−4.045	3.688
O6A	−4.591	0.232	−1.899
H1	−3.703	−1.570	3.546
H2	−2.888	−3.475	2.400
H3	−0.179	−2.332	2.550
H4	−1.845	−2.896	0.141
H5	−1.231	−0.214	1.290
H6A	−1.591	−0.111	−1.061
H6B	−2.993	0.485	−0.285
H2'1	−2.541	−4.509	6.493
H2'2	−1.188	−5.316	5.816
H2''1	−2.607	−7.235	5.266
H2''2	−3.960	−6.428	5.943
H2'''1	−2.850	−6.397	8.126
H2'''2	−1.498	−7.204	7.449
H2''''1	−3.802	−8.693	6.789
H2''''2	−3.852	−8.371	8.473
H2''''3	−2.499	−9.176	7.795
H3'1	1.104	−6.247	1.556
H3'2	−0.200	−6.710	2.577
H3''1	1.269	−6.584	4.532
H3''2	2.574	−6.120	3.521
H3'''1	2.412	−8.255	2.332
H3'''2	1.107	−8.718	3.343
H3''''1	3.236	−7.916	5.009
H3''''2	3.863	−9.020	3.857
H3''''3	2.577	−9.483	4.866
H6'1	−5.259	−2.766	−1.813
H6'2	−4.244	−2.533	−3.175
H6''1	−5.804	−0.862	−4.054
H6''2	−6.819	−1.095	−2.692
H6'''1	−7.146	−3.435	−3.334
H6'''2	−6.131	−3.203	−4.696
H6''''1	−8.103	−1.187	−4.744
H6''''2	−8.899	−2.689	−4.513
H6''''3	−7.883	−2.457	−5.875
O4(2)	−1.926	−0.626	3.760

Table 4 Cartesian coordinates (in Å) of basic residue of ATisoB (4/3 helix)

	X	*Y*	*Z*
O4	0.000	−1.342	0.000
C1	−2.432	−0.063	3.104
C2	−2.637	−1.508	2.656
C3	−1.477	−1.978	1.739
C4	−1.237	−1.013	0.634
C5	−1.108	0.412	1.162
C6	−1.027	1.436	0.050
C2A	−3.991	−3.052	3.834
C2'M	−4.000	−3.934	5.040
C2''M	−5.278	−4.792	5.040
C2'''M	−3.958	−3.066	6.312
C3A	−1.085	−4.319	1.848
C3'M	−1.561	−5.612	1.268
C3''M	−0.846	−6.784	1.967
C3'''M	−1.256	−5.642	−0.241
C6A	−1.292	3.775	−0.254
C6'M	−1.263	5.074	0.487
C6''M	−1.709	6.210	−0.452
C6'''M	−2.220	5.000	1.691
O2	−2.841	−2.346	3.785
O3	−1.758	−3.289	1.295
O6	−0.974	2.761	0.580
O2A	−4.859	−2.962	3.009
O3A	−0.236	−4.182	2.687
O6A	−1.558	3.620	−1.413
H1	−3.302	0.255	3.600
H2	−3.508	−1.542	2.069
H3	−0.610	−2.019	2.385
H4	−2.026	−1.074	−0.057
H5	−0.245	0.481	1.756
H6A	−1.866	1.342	−0.575
H6B	−0.159	1.260	−0.514
H2'1	−3.159	−4.562	5.019
H2'2	−5.284	−5.412	5.888
H2''1	−5.303	−5.384	4.173
H2''2	−5.382	−5.342	4.152
H2'''1	−3.956	−3.687	7.159
H2'''2	−4.801	−2.441	6.338
H2'''3	−3.087	−2.480	6.307
H3'1	−2.597	−5.699	1.415
H3'2	−1.181	−7.692	1.559
H3''1	−1.058	−6.762	2.995
H3''2	0.191	−6.698	1.822
H3'''1	−1.579	−6.555	−0.646
H3'''2	−0.222	−5.537	−0.391
H3'''3	−1.760	−4.852	−0.715
H6'1	−0.287	5.262	0.862
H6'2	−1.688	7.122	0.068
H6''1	−2.685	6.022	−0.791
H6''2	−1.057	6.261	−1.273
H6'''1	−2.199	5.912	2.211
H6'''2	−1.917	4.224	2.332
H6'''3	−3.195	4.813	1.352
O4(2)	−1.342	0.000	4.025

Table 5 Cartesian coordinates (in Å) of basic residue of ATAII (9/2 helix)

	X	Y	Z
O4	0.000	−1.829	0.000
C1	−2.797	−0.829	2.901
C2	−2.572	−2.322	2.680
C3	−1.285	−2.568	1.900
C4	−1.298	−1.771	0.600
C5	−1.601	−0.304	0.891
C6	−1.781	0.535	−0.360
C2A	−3.425	−4.021	4.096
C2M	−3.221	−4.655	5.433
C3A	−0.294	−4.684	2.341
C3M	−0.374	−6.129	1.965
C6A	−3.444	0.981	−1.993
C6M	−4.494	0.305	−2.815
O2	−2.561	−2.994	3.935
O3	−1.177	−3.968	1.612
O5	−2.816	−0.177	1.648
O6	−2.864	0.080	−1.173
O2A	−4.220	−4.353	3.261
O3A	0.429	−4.200	3.167
O6A	−3.152	2.139	−2.031
H1	−3.735	−0.700	3.355
H2	−3.375	−2.695	2.115
H3	−0.464	−2.269	2.483
H4	−2.017	−2.165	−0.056
H5	−0.811	0.098	1.454
H6A	−0.893	0.524	−0.920
H6B	1.978	1.525	−0.070
H2'1	−3.895	−5.452	5.550
H2'2	−3.385	−3.944	6.187
H2'3	−2.238	−5.017	5.501
H3'1	0.316	−6.678	2.535
H3'2	−0.151	−6.239	0.944
H3'3	−1.344	−6.486	2.151
H6'1	−4.945	1.006	−3.454
H6'2	−5.221	−0.112	−2.182
H6'3	−4.052	−0.456	−3.388
O4(2)	−1.801	−0.318	3.778

conformations lies between 3.6 and 4.1 Å. The torsion angles (*Table 6*) that determine the relative position of two successive monomeric units Φ (H1–C1–O4–C4(2)) and Ψ (C1–O4–C4(2)–H4(2)) are very close for the same type of helix, although the fibre repeat might differ to some extent. All the Φ, Ψ values of *Table 6* can be placed in one low-energy region within the -1 kcal mol^{-1} contour of the potential energy map in Figure 4 of ref. 9.

The length and size of the side group strongly influences the helical structure of the main chain. ATAI, the regular modification of crystalline amylose triacetate, forms a 14/11 helix with a non-integral number of residues per left-handed turn of 4.67. ATAII, the high-temperature modification, can be approximated by 4.5 residues per turn. A prolongation in the ester group by a methylene unit which leads to ATP and successively to ATB and ATV exhibits 5 residues per left-handed turn. The replacement of a straight ester group by a bulkier one, as in ATisoB, leads to a conformation with 4 residues per left-handed turn.

The best rotational position of O6 was found to be in the vicinity of *gt** for ATisoB and *gg* for the single chain conformation for all the other four esters investigated in this study[10], although only *tg* positions were allowed in the packing studies of amylose derivatives[2] with the

* *gt* means the bond C6–O6 is *gauche* to O5–C5 and *trans* to C4–C5; *gg* and *tg* are defined correspondingly

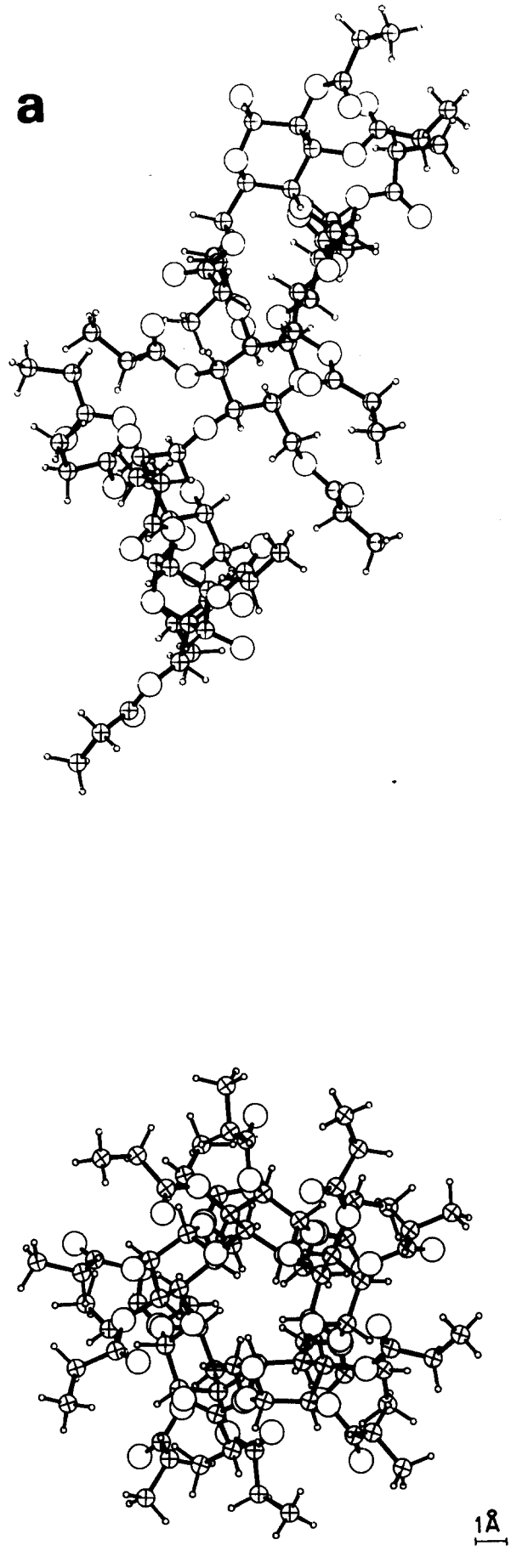

Figure 2 Two projections of 5/4 helices of (a) ATP along the chain axes (*top*) and perpendicular to the chain axes (*bottom*)

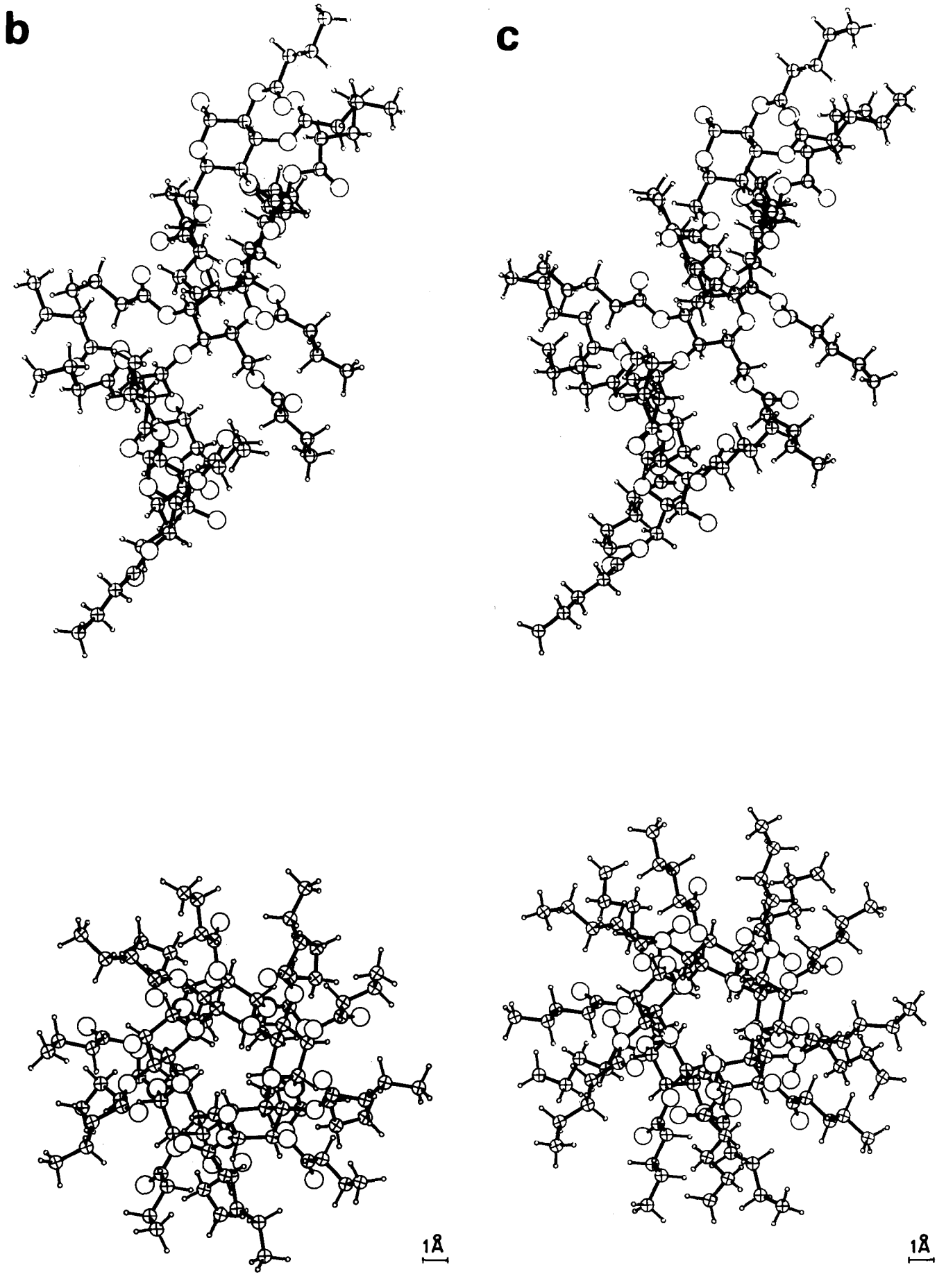

Figure 2 (continued) Two projections of 5/4 helices of (b) ATB and (c) ATV along the chain axes (*top*) and perpendicular to the chain axes (*bottom*)

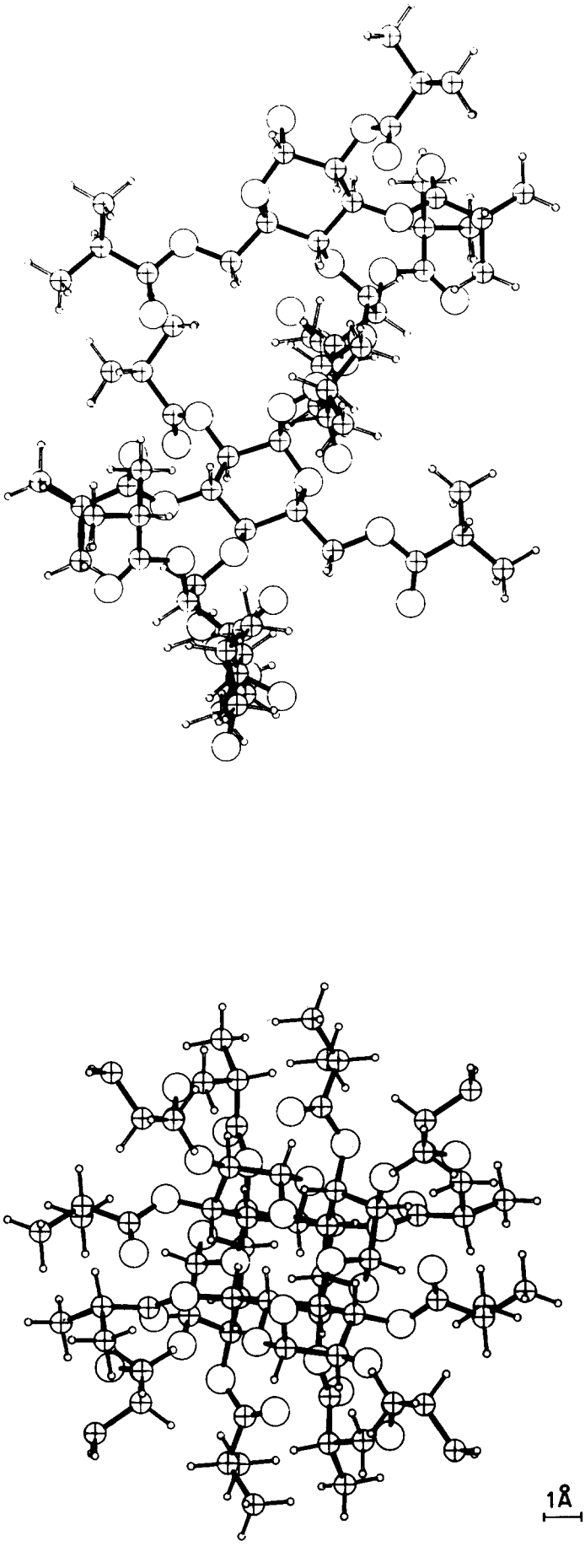

Figure 3 Two projections of a 4/3 helix of ATisoB along the chain axis (*top*) and perpendicular to the chain axis (*bottom*)

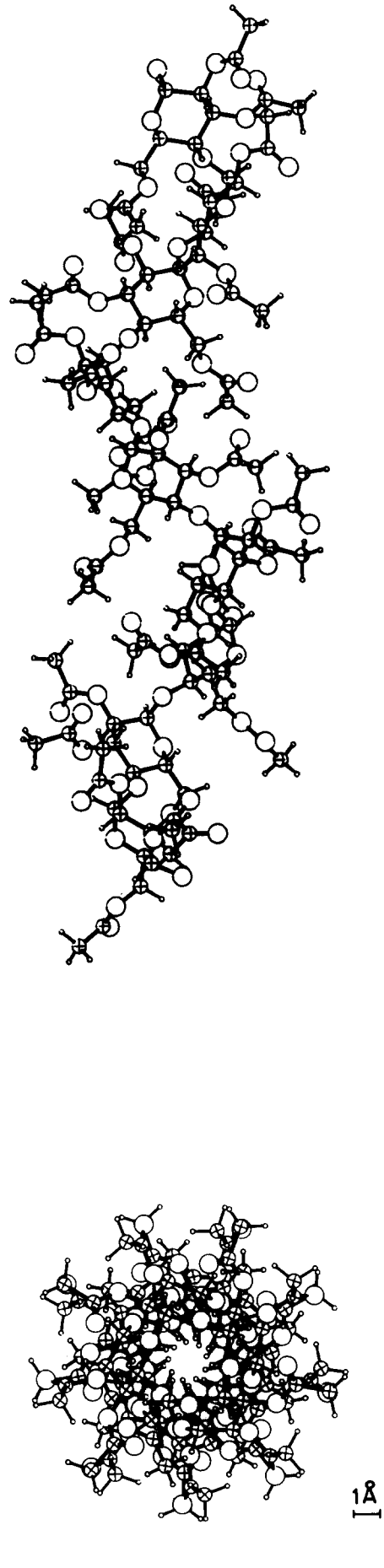

Figure 4 Two projections of a 9/7 helix of ATAII along the chain axis (*top*) and perpendicular to the chain axis (*bottom*)

Table 6 Characteristic values for some amylose derivatives

Amylose derivative	Fibre repeat, *c* (Å)	Rise per residue (Å)	Helix type	Torsion angles (deg)	
				Φ (H1–C1–O4–C4(2))	Ψ (C1–O4–C4(2)–H4(2))
ATAI[3]	52.53	3.75	14/11	−39	−50
ATAII	34.00	3.78	9/7	−48	−33
ATP	18.46	3.69	5/4	−41	−32
ATB	18.45	3.69	5/4	−40	−32
ATisoB	16.10	4.03	4/3	−58	−42
ATV	18.80	3.76	5/4	−37	−35
ATBenz[7] [a]	18.60	3.72	5/4	−41	−32
TEA[8] [b]	15.48	3.87	4/3	−56	−40
TMA–C[6] [c]	15.96	3.99	4/3	−61	−37

[a] A TBenz, amylose tribenzoate; [b] TEA, triethylamylose; [c] TMA–C, trimethylamylose–chloroform complex

exception of trimethylamylose (TMA). The basic unit of TMA is a dimer with O6 in the vicinity of *gt* in one unit and *tg* in the second one.

The helix groove seems to be the hydrophobic site of the molecules of amylose triesters, as only hydrogen atoms point towards the centre of the projection down the helix axes (*Figures 2–4*; bottom).

The loss of reflections and clearness of the X-ray pattern for ATV (*Figure 1f*) is in contrast to all the other patterns of *Figure 1* and is caused by low crystallinity.

CONCLUSIONS

Five amylose triesters have been prepared and the single chain conformation determined by X-ray investigations combined with a model simulation on a computer. Left-handed 5-fold (5/4) helices were proposed for the first time for amylose derivatives and are present in the crystalline regions of ATP, ATB and ATV. The conformation of the triesters ATAI and ATAII as well as ATisoB differs from this helix type and shows a strong influence of the side groups on the main chain that has been considered negligible for polymers. A ninth- and fourth-order meridional reflection in *Figures 1b* and *1h*, respectively, indicates an approximate 9/7 helix for ATAII and a 4/3 helix for ATisoB. The rise per residue falls between 3.7 and 4.1 Å and seems to be invariant for all amylose derivatives[2].

REFERENCES

1 Sarko, A. and Marchessault, R. H. *Science* 1966, **154**, 3757
2 Sarko, A. and Zugenmaier, P. *ACS Symp. Ser.* No. 141 (Eds. A. D. French and K. H. Gardner), American Chemical Society, Washington, 1980, p. 459
3 Sarko, A. *Doctoral Thesis*, State University College of Forestry, Syracuse, New York, 1966
4 Zugenmaier, P. and Sarko, A. *ACS Symp. Ser.* No. 141 (Eds. A. D. French and K. H. Gardner), American Chemical Society, Washington, 1980, p. 225
5 Zuppinger, P. *Doctoral Thesis*, University of Geneva, 1946
6 Büchele, Ch. and Zugenmaier, P. *Colloid Polym. Sci.* 1980, **258**, 768
7 Gutknecht, W. *Diploma Thesis*, Institute for Physical Chemistry, Clausthal Technical University, 1983
8 Bluhm, T. L., Rappenecker, G. and Zugenmaier, P. *Carbohydr. Res.* 1978, **60**, 241
9 Brisse, F., Marchessault, R. H., Pérez, S. and Zugenmaier, P. *J. Am. Chem. Soc.* 1982, **104**, 7470
10 Steinmeier, H. *Diploma Thesis*, Institute for Physical Chemistry, Clausthal Technical University, 1983
11 Husemann, E. and Bartl, H. *Makromol. Chem.* 1956, **18/19**, 342